Chemical Science Review and Letters ISSN 2278-6783

Research Article

Mussaenda erythrophylla Leaves as Effective Green Corrosion Inhibitor of Carbon Steel

Aphouet A. Koffi[1,2,]*, Srinivasan Muralidharan[2] and Albert Trokourey[1]

[1]Labotatoire de Chimie-Physique, Université Félix Houphouët-Boigny, Abidjan-Cocody, 22 B.P. 582 Abidjan 22 CÔTE D'IVOIRE.
[2]Corrosion and Materials Protection Division, CSIR-Central Electrochemical Research Institute, (CECRI) Karaikudi-630003, Tamilnadu, INDIA

Abstract

The performance of *Mussaenda erythrophylla* leaves extract (MELE) as a corrosion inhibitor for carbon steel in 1 M hydrochloric acid was evaluated using mass loss measurements as well as potentiodynamic polarization and electrochemical impedance spectroscopy (EIS) measurements. It was found that the effectiveness of inhibition increased with MELE concentration, in the temperature range 30-45°C. Polarization measurements showed that MELE acts as a mixed-type inhibitor. MELE does not affect the corrosion mechanism. Thermodynamic parameters indicated the physical adsorption of MELE on carbon steel surface. It is also shown that the adsorption behavior of the extract on the carbon steel surface followed the Langmuir isotherm. The inhibition effect of the chemical constituents of MELE on carbon steel surface was confirmed by Fourier transform infrared (FTIR) spectroscopy and atomic force microscopy (AFM).

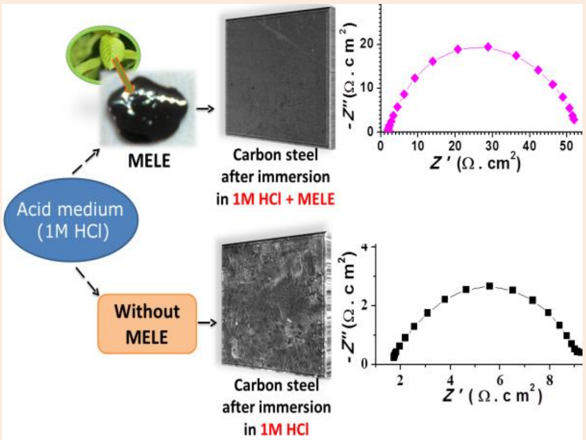

Keywords: *Mussaenda erythrophylla* Leaves Extract; Carbon Steel; EIS; FTIR; Adsorption

***Correspondence**
Aphouet A. Koffi
Email: koffiaphouet@yahoo.fr

Introduction

Corrosion is termed as the chemical or electrochemical reaction between a material and its environment that leads to deterioration of the material and/or its properties [1] thereby generating a considerable economic cost [2]. In industries, corrosion is mostly caused by the use of acid solutions in the pickling of metallic structures, acidization of oil wells and in the cleaning of scales. In these processes, inhibitors are generally used to control the metal dissolution as well as acid consumption [3]. Researchers have shown that the most effective inhibitors are the organic compounds with π bonds and heteroatoms (P, S, N, and O), and the inorganic compounds, such as chromate, dichromate and nitrite. However, the toxic effects of some inhibitors, especially the inorganic compounds, have led to the use of materials as anticorrosion agents which are eco-friendly and harmless [4, 5].

In addition to being non-polluting and environmentally acceptable, plant extracts are inexpensive, readily available and inexhaustible sources. Plant extracts are viewed as an incredibly rich source of naturally synthesized chemical compounds that can be extracted by simple procedures with low cost [6]. Several leaves extracts [7-10], as well as other parts of plant [11-18] have been reported as good corrosion inhibitors of various metals in acid medium. The inhibitory action of these plant extracts is due to the presence of organic compounds such as saponins, tannins, alkaloids, steroids, glycosides and amino acid [7].

Mussaenda erythrophylla (Rubiaceae) is native to western tropical Africa, occasionally seen in gardens and parks as an ornamental plant in India and is commonly known as mussenda (Telugu), nagavalli (Sanskrit) and red flag bush (English). The roots are used for treating cough, jaundice and when chewed acts as an appetizer. A number of triterpenoids, saponins, iridoid and glycosides as component were reported [19, 20]. The pharmacological activities reported from Mussaenda species are diuretic, antiphlogistic, antipyretic and effective in laryngopharyngitis, acute gastroenteritis, dysentery, anti-fertility and antiurolithiatic [20, 21].

However, to the best of our knowledge, there is no report on this plant as a corrosion inhibitor. The aim of this work is to study the leaves of *Mussaenda erythrophylla*, as green corrosion inhibitor on carbon steel in hydrochloric acid solution.

Experimental

Materials and Reagents

The material used in this study was carbon steel with chemical composition in weight %: C = 0.18, Si = 0.03, P = 0.06, S = 0.05, Mn = 0.12 and Fe as remaining component. The aggressive medium (1M hydrochloric acid) was prepared by dilution of an analytical reagent (RANKEM) grade 35% with distilled water. Acetone (Laboratory Reagent) was purchased from RANKEN and used as received.

The leaves of *Mussaenda erythrophylla* were picked in the research center CSIR-CECRI Karaikudi. The inhibitors were extracted from these leaves. Ethanol, absolute (Analytical Reagent) and petroleum ether (60-80°C, Guaranteed Reagent) were used for the extraction of MELE. 100-400 mg L^{-1} of MELE was used, made by dissolving in the acid solution.

Extraction procedure of MELE

The leaves of *Mussaenda erythrophylla* were cleaned with tap water to eliminate dust. They were then dried in shade at room temperature, to enrich the active constituents [3, 22]. The dried leaves were crushed into fine particles, and extracted in an ethanol–water (80/20 v/v %) mixed solvent, using soxhlet apparatus (Borosil 500 mL). Appearance of colorless solvent in the siphon tube of soxhlet apparatus was taken as the end point of the extraction. The solution was concentrated to about 100 mL, and was then degreased with petroleum ether. The alcoholic stage was thereafter extracted with a separating funnel. The extract was again concentrated to about 50 mL using a distillation unit, and finally dried in vacuum drying oven at 60°C for 3 days. After complete drying, a dark brown solid residue (MELE) was obtained, and preserved in desiccator.

Gas Chromatography-Mass Spectroscopy (GC-MS) analysis of MELE

10 mg of MELE was dissolved in 10 mL of alcohol. The solution was filtered, centrifuged (20 min, 10000 rpm/min) and filtered again. 1µL of the obtained solution was employed for the analysis.

The volatile compounds of the extract were identified using a gas chromatography coupled to mass spectroscopy. The analysis was performed on a chromatograph Agilent Technologies, interfaced to a mass spectrometer model No. 5975C Inert MSD with Triple Axis detector. The column used was a capillary column DB5 fused silica (30 m × 0.25 mm ID × 0.25 micron). Helium was used as the carrier gas at a constant flow of 1 mL / min. An injection volume of 1 mL electron ionization was employed (split ratio 10: 1). The temperature of the ejector was 275ºC; the detector temperature was 280°C. The oven temperature was programmed as follows: 110 ° C for 2 min, with an increase of 10°C / min to 200°C, holding at 200°C for 9 min; then increase up to 280ºC at a rate of 5ºC / min and ending with a 2 min isothermal at 280ºC. A scan interval of 0.5 s and fragments of 20 to 600 Da has been applied.

Interpretation of GC-MS results was done using the database of National Institute Standard and Technology (NIST), by comparing the mass spectrum of the compounds to be identified with the spectrum of the known compounds stored in the NIST library.

Weight loss measurements

The carbon steel samples of size 2 cm × 4 cm (and thickness 0.05-0.25 cm) were abraded with various grades of emery paper until a mirror finish, then washed with distilled water, degreased with acetone, and finally dried in air. The samples, in triplicate, were accurately weighed and immersed in hydrochloric acid solution without or with plant extract. After 1 hour, the three specimens were taken out from the solution and thoroughly washed with distilled water. They were air dried, and reweighed. From the weight loss, corrosion rate (v) in mg cm^{-2} h^{-1} was calculated using the following equation:

$$v = W/(S \times t) \tag{1}$$

W is the average weight loss (mg), S the average area (cm^2), and t the immersion time (h).

The inhibition efficiency η_W (%) and surface coverage θ_W were calculated as follows:

$$\eta_W\ (\%) = [(v_o - v)/v_o] \times 100 \quad (2)$$

$$\theta_W = (v_o - v)/v_o \quad (3)$$

where v_o and v are the rates of corrosion in the absence and presence of MELE respectively.

Electrochemical measurements

Potentiodynamic polarization and electrochemical impedance spectroscopy (EIS) were performed in a conventional three electrode cell assembly. This electrochemical cell was made with a platinum foil (1 cm^2) counter electrode (CE), a saturated calomel electrode (SCE) as reference electrode and carbon steel specimen as working electrode (WE). The specimens were cut from carbon steel sheets and embedded in epoxy resin leaving only a surface area of 1 cm^2. The exposed surface was prepared as described in the previous section.

All measurements were carried out on Gill AC Model 1566 electrochemical instrument. Before each measurement the WE was immersed in the test solution for 1 h to achieve a steady state. After the open circuit potential (OCP) was determined, EIS measurements were performed in a frequency range of 100 kHz to 0.01 Hz with 10 mV AC amplitude. Inhibition efficiency η_{EIS} (%) was obtained from the following relation:

$$\eta_{EIS}\ (\%) = (R_{ct(inh)} - R_{ct(o)}) / R_{ct(inh)} \times 100 \quad (4)$$

where $R_{ct(o)}$ and $R_{ct(inh)}$ are charge transfer resistances for carbon steel in uninhibited and inhibited solution, respectively.

Thereafter, anodic and cathodic polarization curves were recorded from -200 mV to + 200 mV relative to the open circuit potential with a sweep rate of 1mV s^{-1}. Inhibition efficiency η_P (%) is defined as follows:

$$\eta_P\ (\%) = (i_{corr} - i_{corr(inh)}) / i_{corr} \times 100 \quad (5)$$

where i_{corr} and $i_{corr(inh)}$ represent the corrosion current density values without and with MELE, respectively.
Each experiment was repeated at least three times to check the reproducibility in aerated condition.

Fourier transform infrared (FTIR) and atomic force microscopy (AFM) characterizations

The compounds extracted from the leaves of *Mussaenda erythrophylla*, and the thin layer formed on the metal surface was characterized by FTIR spectroscopy. The samples were prepared using potassium bromide (KBr) pellet and spectra were recorded in a BRUKER spectrophotometer (TENSOR 27 model, Opus-6.5 version) by scanning the samples through a wave number range of 4000 to 400 cm^{-1}.

Further characterization of the uninhibited and inhibited carbon steel surfaces with respect to surface roughness was done by AFM. The experiments were performed by contact mode (Agilent Technologies, Picoview 1.12.2).

Results and Discussion

Characterization and identification of MELE compounds

FTIR spectroscopy was used to determine the functional groups present in MELE. As displayed in **Figure 1(a)**, a very strong broad band at 3403.71 cm^{-1} is attributed to O–H stretching [18, 23, 31] while the band at 2931.04 cm^{-1} could be assigned to $–CH_2$ asymmetrical stretching vibration [18]. The absorption band at 2113.15 cm^{-1} and the peak at 1696.13 cm^{-1} could be associated to the terminal alkyne $C\equiv C$-H stretching vibration and C=O stretching vibration respectively [18, 31]. The bands at 1610.76, 1520.43 and 1447 cm^{-1} can be assigned to the aromatic ring stretching vibration [18, 23]. Furthermore, the peak at 1376.01 cm^{-1} is attributed to C–H bending band in $–CH_3$ [18]. Besides, the absorption bands at 1064.24 cm^{-1} and 1275.21 cm^{-1} could be assigned to the C–O–C stretching vibration [18, 23]. The bands below 1000 cm^{-1} correspond to the aliphatic and aromatic C–H groups [9]. These results indicate that MELE contains C and O atoms in functional groups (O-H, C=C, C=O, $C\equiv C$, C-O) and aromatic ring.

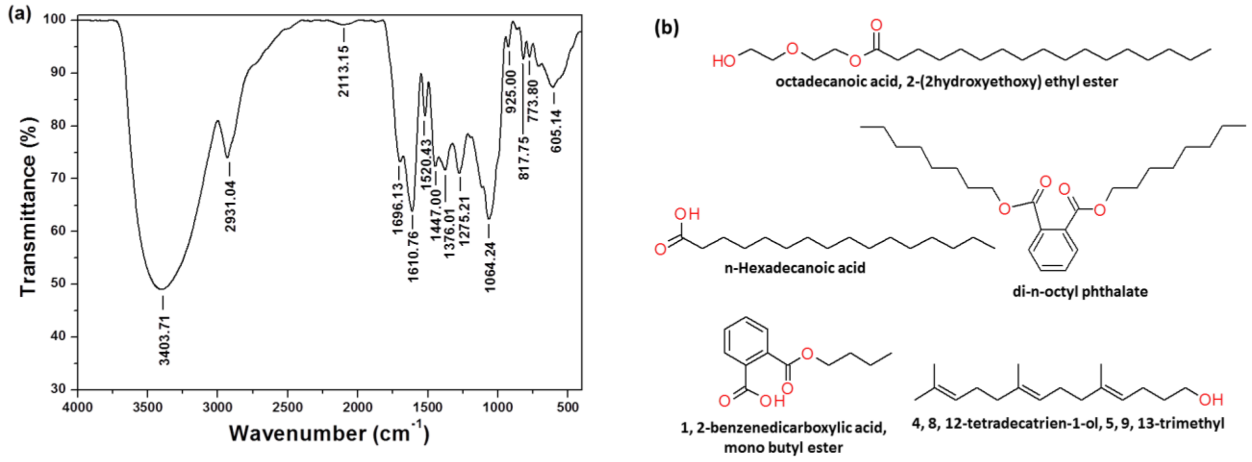

Figure 1 (a) FT-IR spectra and **(b)** chemical structure of the identified components of MELE

GC-MS was used to identify the volatile compounds of MELE. The chemical structures of the identified compounds are represented in **Figure 1(b)**. The results are in agreement with those of FTIR.

Weight loss data

To evaluate the efficiency of MELE as corrosion inhibitor, mass loss was investigated from 30°C to 45°C. The mass loss of carbon steel immersed in the test solution expressed as corrosion rate is shown in **Figure 2(a)**. As observed in this figure, a decrease in corrosion rate in the presence of MELE is obtained at all the temperatures. This behavior expresses clearly that MELE has inhibitory effect on the corrosion of carbon steel in hydrochloric acid at the studied temperatures. This inhibitory effect is due to the adsorption of MELE constituents on the metal surface [24, 29].

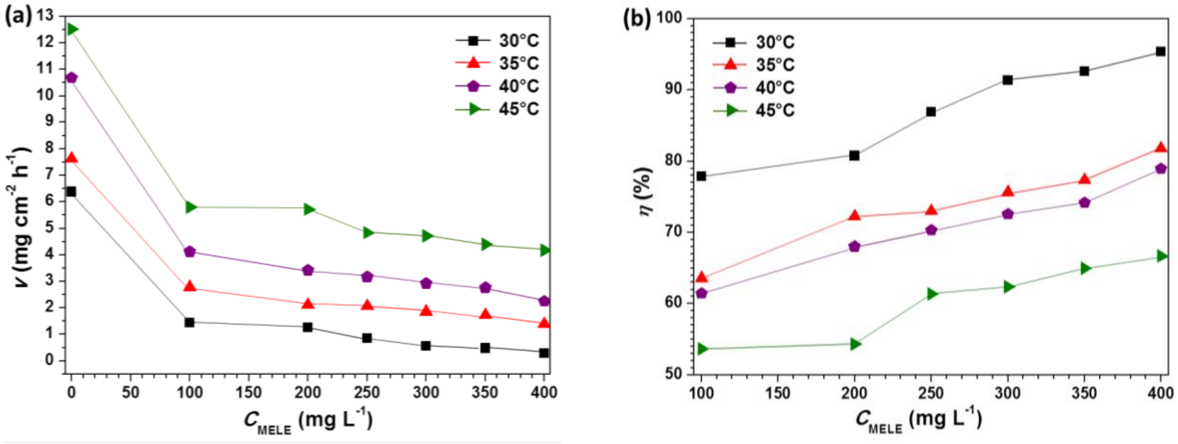

Figure 2 Plots of **(a)** corrosion rate *v* (mg cm^{-2} h^{-1}) of carbon steel immersed in 1M HCl, and **(b)** inhibition efficiency η_w (%) of MELE

On the other hand, the inhibitory efficiency was plotted against the concentration of the plant extract (**Figure 2(b)**). The results show an increase in the efficiency with the increase of the concentration of the plant extract at all the temperatures studied, probably due to the strengthening of the barrier formed by the inhibitor molecules. However, it can be noticed that the rise in the temperature causes a decrease in inhibition efficiency of MELE, due to desorption of some inhibitory species. Indeed, the increase in temperature having increased kinetic energy of the metal surface, the adsorption process is weakened. The degree of adsorption decreases with increasing temperature, while the desorption increases [25]. These results highlight the dependence of the corrosion rate as well as inhibitory efficacy relative to the temperature.

Electrochemical measurements

Tafel polarization studies

Potentiodynamic polarization method was used to define the type of the inhibitor. **Figure 3** depicts the polarization curves of the studied metal in 1M hydrochloric acid (1 M HCl) with different concentrations of the plant extract.

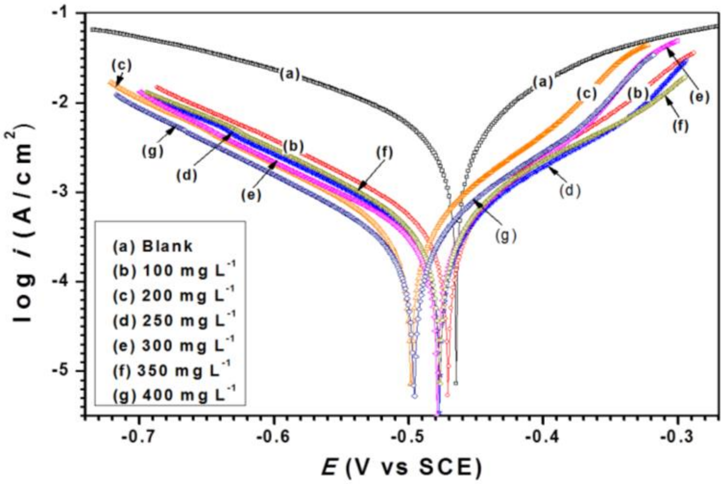

Figure 3 Polarization curves of carbon steel in 1M HCl with different concentrations of MELE at 30 °C

It can be seen that the cathodic and anodic curves are shifted to lower values of the current density in the presence of MELE, thereby inducing a decrease in the corrosion rate of carbon steel. The presence of these green inhibitor molecules considerably reduces corrosion current density. We can also notice the shift of Tafel curves towards cathodic region. These results highlight the inhibitory effect of the plant extract on hydrogen evolution process.

In addition, a difference in the shape of the anodic curves in the presence and absence of MELE is observed towards the high potential, pointing the action of MELE on the anodic reaction. Therefore MELE retards both the hydrogen evolution and the metal dissolution. The difference in the shape could be due to the formation of a barrier film on the metal surface, when MELE is added to the acid solution [31]. The electrochemical parameters derived from the Tafel plots, namely corrosion potential E_{corr}, corrosion current density i_{corr}, anodic and cathodic tafel slopes (b_a and b_c respectively) as well as inhibition efficiencies η_P (%) are given in **Table 1**. The extrapolation of Tafel plots was performed using the Analysis ACM v4 software. The results show that the corrosion current density (i_{corr}) significantly decreases in the presence of MELE. The performance of inhibitory molecules is improved when the concentration of the plant extract increases. One can further note that adding MELE causes a maximum shift in E_{corr} value of +33 mV. This displacement of corrosion potentials (E_{corr}), less than ±85 mV, suggests that the inhibitors are mixed-type [31, 32] that is confirmed by the anodic and cathodic Tafel slopes (b_a and b_c) values.

Table 1 The electrochemical parameters from polarization curves for carbon steel in 1M hydrochloric acid solution containing MELE at 30 °C

C_{MELE} (mg L^{-1})	$-E_{corr}$ (mV vs. SCE)	$-b_c$ (mV dec^{-1})	b_a (mV dec^{-1})	i_{corr} (mA cm^{-2})	η_P (%)
0	465	198	128	8.8	--
100	471	142	100	1.2	83.0
200	498	129	86	1.1	87.5
250	477	143	114	0.9	89.8
300	479	130	75	1	88.6
350	477	131	95	0.8	90.9
400	496	133	91	0.7	92

EIS measurements

The electrochemical impedance measurements were performed to acquire information on the nature of the electrochemical reactions that occurred on the metal surface. Nyquist spectra exhibit similar shape in absence and presence of MELE (**Figure 4(a)**).

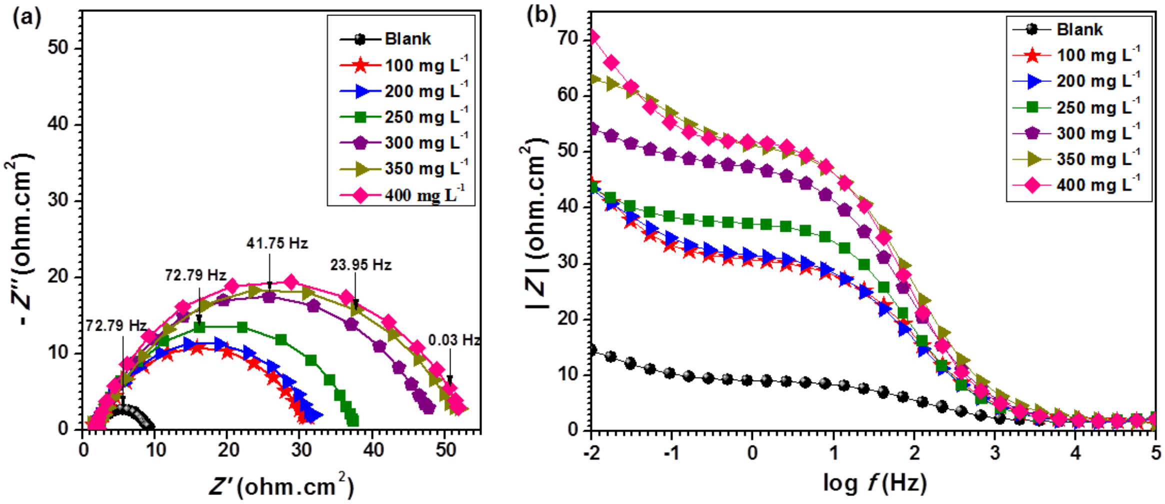

Figure 4 Electrochemical impedance spectra of carbon steel in 1M HCl without and with various concentrations of MELE at 30 °C: **(a)** Nyquist and **(b)** Bode plots.

The curves show a capacitive loop which is larger for the inhibited medium. Capacitive loop is related to charge transfer in the corrosion process of the carbon steel and to the double layer capacitance [7]. The increase in the size of the semicircle diameter in the presence of the extract indicates that a barrier is gradually formed on the carbon steel surface. Further inspection reveals that these capacitive loops are not perfect semicircles. This can be attributed to the frequency dispersion due to the roughness and heterogeneities of the electrode surface [4, 27]. Thorough examination of the curves shows that the barrier is larger with increasing inhibitors concentration. From the foregoing, it is observed that the inhibitors do not affect the corrosion mechanism [27]. From Bode plot, it can be seen that the curves show a characteristic with one time constant (**Figure 4(b)**), corresponding to the capacitance loop. These results suggest that carbon steel has better corrosion resistance in the presence of MELE.

The intersection of the semi-circular curves with the horizontal axis at high frequencies corresponds to solution resistance R_S. The charge transfer resistance R_{ct} was determined by the difference in impedance values at higher and lower frequencies. The double layer behaves as a constant phase element (CPE) rather than a capacitor. Thus, the CPE is substituted for the interfacial capacitance to fit more exactly the semicircle.

C_{dl} was computed from the formula [32] given below:

$$C_{dl} = (Y_o\, R_{ct}^{(1-n)})^{(1/n)} \qquad (6)$$

where Y_o is the magnitude of the CPE and n is the CPE exponent which quantifies different physical phenomena at the metal surface.

The values obtained by fitting the Nyquist diagram to the equivalent circuit model R_S-$Q_{dl}\,|R_{ct}$, using WonATech ZMAN^{TM} 2.2 software, are summarized in **Table 2**. The values of the inhibition efficacy are also shown in Table 2. Analysis of these data clearly indicates that the charge transfer resistance raises with increased concentration of the inhibitor molecules, while the capacitance reduces. A large R_{ct} is attributed with a lower corroding system, and the protection offered by the plant extract is associated with a drop of C_{dl} [27]. The decrease in C_{dl} values as well as Y_o values indicates moreover the reduction of charges accumulated in the double layer due to the formation of the adsorbed layer of the inhibitors. In contrast, the value of n increases with the addition of inhibitors which shows that the presence of inhibitors reduces the corrosive attack of the aggressive environment, hence a less rough surface. Based on these results, it could be concluded that the inhibitor molecules function by adsorption at the metal/solution interface, thereby delaying the dissolution of carbon steel in the hydrochloric acid solution (1M HCl).

Table 2 EIS parameters for the corrosion of carbon steel in 1 M HCl solution containing MELE at 30 °C

C_{MELE} (mg L^{-1})	CPE (10^{-6} Ω cm^{-2} s^n)	*n*	R_{ct} (Ω cm^2)	C_{dl} (μF cm^{-2})	η_{EIS} (%)
0	1349	0.74	7.8	273	--
100	281	0.79	29.6	79	73.6
200	269	0.81	30.4	87	74.3
250	219	0.83	35.8	81	78.2
300	171	0.84	45.8	68	83
350	272	0.74	52.3	60	85
400	155	0.84	49.8	61	84

Adsorption isotherm

The adsorption isotherms are very useful tool to define the interactions between the adsorbed species and the surface of the metal [24]. Various isotherms have been applied to the adsorption of MELE constituents in order to determine the most appropriate model. **Figure 5** shows the Langmuir equation model:

$$C_{inh}/\theta = 1/K + C_{inh} \qquad (7)$$

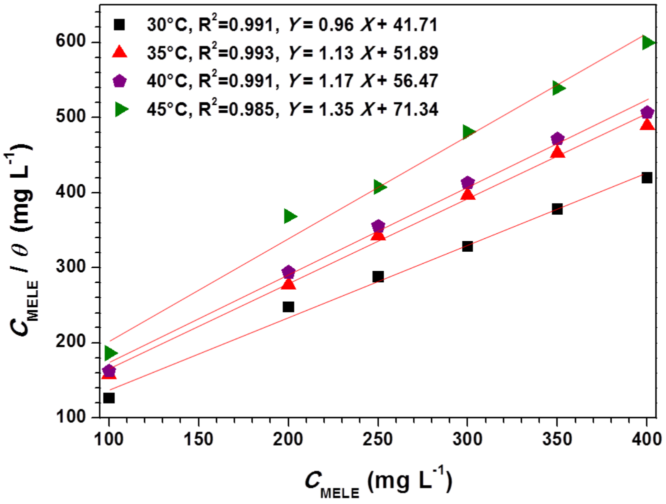

Figure 5 Langmuir isotherm applied to the adsorption of MELE molecules on the carbon steel surface in 1M HCl

Linear correlation coefficients, all close to unity showed that this model is appropriate to explain the adsorption in this study. However, the slight deviation from unity indicates interactions between adsorbed species. In fact, species which adsorb on the metal surface possess polar functional groups and aromatic ring. The value of the slope is less than unity due to the multilayer formation of inhibitors at 30 °C. For higher temperatures, the values are larger than unity which supports the fixation of species on several adsorption sites of the metal [11, 15, 35].

Activation parameters

The corrosion rate can be related to the temperature by the Arrhenius equation [35].

$$v = A \exp[- E_a^*/(RT)] \qquad (8)$$

where *v* represents the corrosion rate of carbon steel, A a pre-exponential factor, E_a* the apparent activation energy, *R* the gas constant and *T* the absolute temperature.

The plot of log *v* as a function of 1/*T* (**Figure 6(a)**) gives a straight line of slope -(E_a*)/2.303*R* from which the activation energy E_a* is derived. The values of E_a* are shown in **Table 3**. It is noted that the presence of MELE causes an increase in the activation energy which suggests that the inhibitory species are physically adsorbed on the metal surface [36].

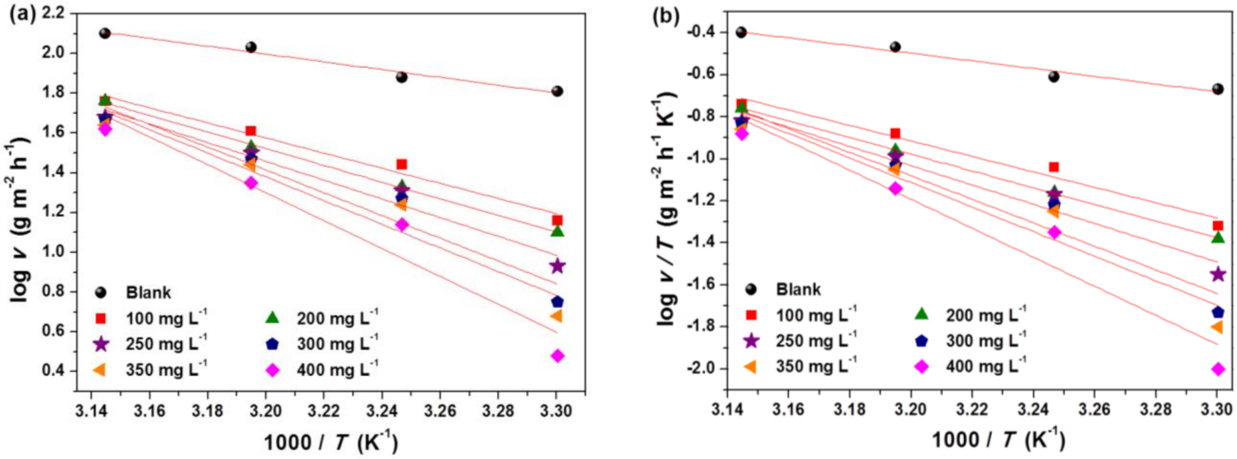

Figure 6 Arrhenius plots **(a)** log *v* versus 1000/*T* and **(b)** log *v*/*T* versus 1000/*T*

Table 3 Activation parameters

C_{MELE} (mg L^{-1})	E_a* (kJ mol^{-1})	ΔH_a (kJ mol^{-1})	ΔS_a (kJ mol^{-1}K^{-1})
0	37.62	35.04	-95
100	72.84	70.27	6.73
200	80.42	76.01	26.96
250	90.26	87.69	63.23
300	109.58	106.99	124.08
350	114.06	111.84	138.99
400	134.39	132.17	202.52

The dependence of the corrosion rate with the temperature can be expressed by another Arrhenius formula.

$$v = RT/Nh \exp(\Delta S_a/R) \exp(-\Delta H_a/RT) \qquad (9)$$

N is Avogadro number (6.022.10^{23} mol^{-1}) and *h* Planck constant (6.626.10^{-34}J s)

From the plot of the curve log *v*/*T* as function of 1/*T*, variations of activation enthapy ΔH_a and activation entropy ΔS_a can be determined. **Figure 6(b)** shows the straight line with slope -ΔH_a/2.303*R* and intercept (log *R*/*Nh* + ΔS_a/2.303*R*). The values of ΔH_a (Table 3) are positive, indicating the endothermic nature of the corrosion process. The values of ΔS_a are also recorded in Table 3. These values indicate that the disorder has increased in the presence of MELE molecules, and that increases with increasing concentration of inhibitors. This can be explained by the fact that the formation of the activated complex Fe–H_2O follows a dissociative mechanism [37, 38].

Metal surface analysis

Figure 7 shows FTIR spectrum of the carbon steel surface after its immersion in 1M HCl with 400 mg L^{-1} of plant extract.

As can be seen, most of the peaks of MELE spectrum are also present in those of the metal surface, but with some changes. The peak at 3403.71 cm^{-1} attributed to O–H stretching bond was shifted to 3357.03 cm^{-1}. The -CH_2 stretching vibration decreased from 2931.04 cm^{-1} to 2917.54 cm^{-1}. The frequencies of vibration 1610.76 cm^{-1} and 1447 cm^{-1} of the aromatic ring have shifted to 1635.02 cm^{-1} and 1417.89 cm^{-1}, respectively. The adsorption band of C–O–C group has moved from 1064.24 cm^{-1} to 1092.62 cm^{-1}. The displacements of the peaks clearly indicate that the functional groups O–H and C–O and the aromatic ring of MELE constituents are directly involved in complex Fe^{2+}–MELE formation [9, 39]. These results confirm the presence of an inhibitor adsorbed film on the surface of carbon steel, responsible for the enhanced protection of the metal against corrosion.

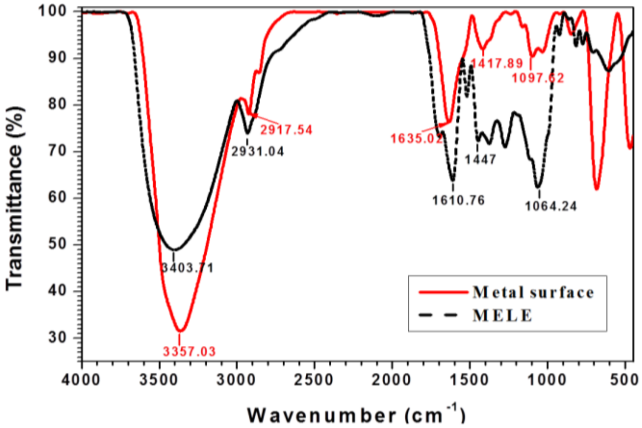

Figure 7 FTIR spectra of MELE and the film formed on the metal surface

The topography of carbon steel surface after immersion in hydrochloric acid in the presence of 400 mg L^{-1} plant extract (**Figure 8 (b)**) revealed the presence of the thin film formed on the surface of metal, confirming the results of FTIR. This film has a thickness of about 0.7 µm, and it is responsible for the corrosion resistance of carbon steel in the acidic medium.

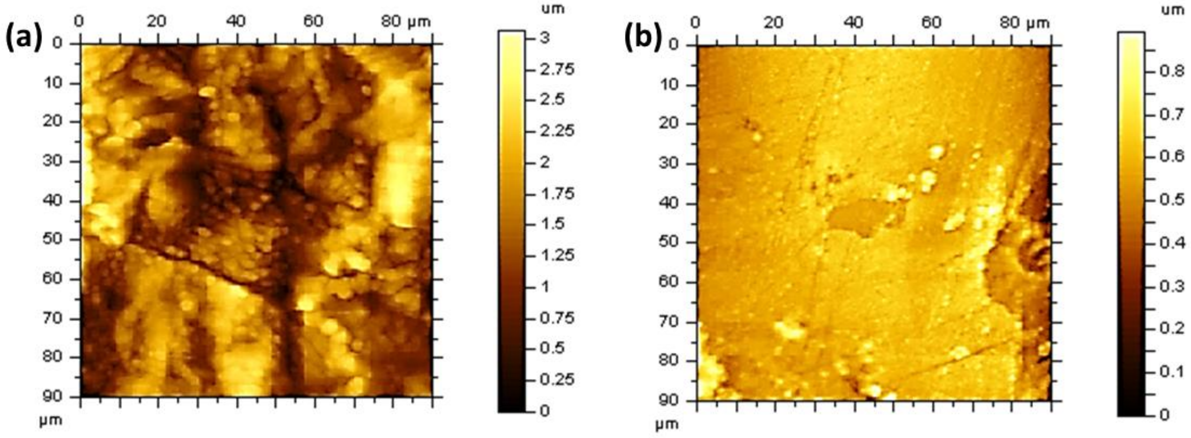

Figure 8 AFM topography of the carbon steel surface after 1h of immersion at 30 °C in 1M HCl **(a)** without and **(b)** with 400 mg L^{-1} of MELE

Mechanism of inhibition

The inhibitory action of MELE is due to the adsorption of its various components, which is consistent with the expected requirements. The FTIR spectrum of the formed film (Figure 7) confirms the interactions between the carbon steel surface and the organic molecules. These inhibitor molecules could therefore adsorb on the metal surface either through the unshared electron pair of oxygen atoms or π-electrons.

MELE constituents may combine with freshly generated Fe^{2+} ions on steel surface thanks to the lone-pair electrons of O atoms, which form metal-inhibitor complexes. These complexes might get adsorbed onto steel surface by van der Waals force to form a protective film which protects carbon steel from corrosion [7, 9].

The adsorption could also happen by protonation of MELE compounds in acidic medium according the following equation:

$$[Org] + x\,H^{+} \rightarrow [OrgH_{x}]^{x+} \qquad (10)$$

Protonated molecules can be adsorbed onto the metal surface, previously charged by the chloride ions. In fact the chloride ions have a great tendency to adsorb to the metal surface, which facilitates the adsorption of cations [8, 33]. Consequently, the inhibition by adsorbed molecules is due to the electrostatic interactions between the ions adsorbed chloride and the protonated compounds of MELE.

Conclusions

The leaves extract of *Mussaenda erythrophylla* has a good inhibitory effect on the corrosion of carbon steel in 1M hydrochloric acid solution. Inhibition efficacy rises with the increase in MELE concentration at the studied temperatures, and reaches a maximum efficiency of 95% for 400 mg L^{-1} of MELE.

MELE is a mixed-type inhibitor. The addition of MELE slows down both anodic and cathodic reactions. MELE does not change the mechanism of corrosion, but rather acts by adsorption on the metallic surface.

The adsorption is spontaneous, exothermic and takes place according to Langmuir model. The adsorption of MELE compounds takes place either through the protonation of the molecules, or by the formation of metal-inhibitors complex. Hence MELE can be used as an inhibitor to reduce acid corrosion of carbon steel.

Acknowledgements

Aphouet A. Koffi thanks the Council of Scientific and Industrial Research (CSIR), India, and The World Academy of Sciences (TWAS) for the award of PG Research Fellowship (Letter dated 05/03/2013, FR number: 3240267285). The authors thank the Director, CSIR-CECRI, Karaikudi for his keen interest in this work. The authors also thank the scientists for making available their equipments, and their helpful suggestions.

References

[1] Banerjee S and Tyagi A (Eds.), Functional Materials-Preparation, Processing and Applications, 12 – Corrosion-Resistant Materials, Vivekanand K, Elsevier, London, USA, 2012, p507–547.
[2] Buchheit RG (Ed.), Handbook of Environmental Degradation of Materials, Chapter 1, Cost of corrosion in the United States, Koch GH, Brongers MPH, Thompson NG, Virmani YP, Payer JH, Elsevier, London, USA, 2005, p3–24.
[3] Chebouat E, Dadamoussa B, Gherraf N, Gouamid M, Allaou M, Cheriti A, Khiari A, Int J Electrochem Sci 2013, 8, 12147– 12153.
[4] Amin MA, Khaled KF, Mohsen Q, Arida HA, Corros Sci 2010, 52, 1684–1695.
[5] Gece G, Corros Sci 2011, 53, 3873–3898.
[6] Chevalier M, Robert F, Amusant N, Traisnel M, Roos C, Lebrini M, Electrochim Acta 2014, 131, 96–105.
[7] Li X, Deng S, Fu H, Corros Sci 2012, 62, 163–175.
[8] Deng S, Li X, Corros Sci 2012, 55, 407-415.
[9] Li L, Zhang X, Lei J, He J, Zhang S, Pan F, Corros Sci 2012, 63, 82–90.
[10] Hamdy A, El-Gendy NSh, Egypt J Pet 2013, 22, 17-25.
[11] Prabhu D, Rao P, J Environ Chem Eng 2013, 1, 676-683.
[12] Afia L, Salghi R, Bammou L, Bazzi El, Hammouti B, Bazzi L, Bouyanzer A, J Saudi Chem Soc 2014, 18, 19-25.
[13] Yaro AS, Khadom AA, Wael RK, Alexan Eng J 2013, 52, 129-135.
[14] Raja PB, Qureshi AK, Rahim AA, Osman H, Awang K, Corros Sci 2013, 69, 292-301.
[15] Uwah IE, Okafor PC, Ebiekpe VE, Arab J Chem 2013, 6, 285-293.
[16] Pereira SSAA, Pêgas MM, Fernández TL, Magalhães M, Schöntag TG, Lago DC, Senna LF, D'Elia E, Corros Sci 2012, 65, 360-366.
[17] Nkuzinna O, Menkiti MC, Onukwuli OD, Int J Multidisciplinary Sci Eng 2011, 2 , 1-5.
[18] Eddy NO, Odiongenyi AO, Ameh PO, Ebenso EE, Int J Electrochem Sci 2012, 7, 7425 – 7439.
[19] Rani BEA and Basu BBJ, Int J Corros 2012, Article ID 380217, 1.
[20] Eswaraiah MC, Satyanarayana T, Int J Pharm Sci Res 2010, 1, 20-26.
[21] Venkatesh K, Rao UU, Kiranmayi GVN, Naik RN, Mukharjee NSV, Vinay VNV, Phanindra K, Int J Bio Pharm Res 2013, 4, 8-10.
[22] Venkatesh K, Kiranmayi GVN, Vinay VNV, Srinivasu M, Naik RN, Rani KL, Int J Adv Pharm Res 2013, 4, 1835-1840.
[23] Anand B, Balasubramanian V, Elixir Corros 2011, 37, 3832-3835.
[24] Kadhum AAH, Mohamad AB, Hammed LA, Al-Amiery AA, San N, Musa AY, Mat 2014, 7, 4335-4348.
[25] Felipe MBMC, Silva DR, Martinez-Huitle CA, Medeiros SRB and Maciel MAM, Mater Corros 2013, doi: 10.1002/maco.201206532.
[26] Abdel-Azim AA, Milad R, El-Ghazawy R, Kamal R, Egypt J Pet 2014, 23, 15-20.

[27] Ahamad I, Prasad R, Quraishi MA, Corros Sci 2010, 52, 1472-1481.
[28] Li X, Deng S, Fu H, Xie X, Corros Sci 2014, 78, 29-42.
[29] Da Silva AB, Gomes JACP, D'Elia E, Rezende MJC, Pinto AC, Silva BNM, Silva BV, Int J Electrochem Sci 2013, 8, 9317-9331.
[30] Li X, Deng S, Fu H, Corros Sci 2011, 53, 302-309.
[31] Bobina M, Kellenberger A, Millet J-P, Muntean C, Vaszilcsin N, Corros Sci 2013, 69, 389-395.
[32] Halambek J, Žutinić A, Berković K, Int J Electrochem Sci 2013, 8, 11201-11214.
[33] Al-Otaibi MS, Al-Mayouf AM, Khan M, Mousa AA, Al-Mazroa SA, Alkhathlan HZ, Arab J Chem 2014, 7, 340-346.
[34] Khamis A, Saleh MM, Awad MI, Corros Sci 2013, 66, 343-349.
[35] Ji G, Dwivedi P, Sundaram S, Prakash R, Ind Eng Chem Res 2013, 52, 10673-10681.
[36] Al Nazeer A, Shalabi K, Fouda AS, Res. Chem. Intermed., doi 10.1007/s11164-014-1570-4.
[37] Solmaz R, Corros Sci 2014, 79, 169-176.
[38] Ji G, Dwivedi P, Sundaram S, Prakash R, Res. Chem. Intermed., doi 10.1007/s11164-015-2029-y.
[39] Faustin M, Maciuk A, Salvin P, Roos C, Lebrini M, Corros Sci 2015, 92, 287-300.
[40] Oguzie EE, Adindu CB, Enenebeaku CK, Ogukwe CE, Chidiebere MA, Oguzie KL, J Phys Chem C 2012, 116, 13603-13615.

Publication History

Received	13th	Oct	2015
Revised	16th	Nov	2015
Accepted	08th	Dec	2015
Online	30th	Dec	2015